Enhanced antiferromagnetic exchange coupling in Fe/Si/Fe epitaxial trilayers with $Fe_{0.5}Si_{0.5}$ boundary layers

R. R. Gareev,[a] D. E. Bürgler, M. Buchmeier, R. Schreiber, and P. Grünberg
Institut für Festkörperforschung, Forschungszentrum Jülich GmbH, D-52425 Jülich, Germany

(Received 1 April 2002; accepted for publication 14 June 2002)

Epitaxial $Fe/Fe_{0.5}Si_{0.5}$/Si-wedge/$Fe_{0.5}Si_{0.5}$/Fe structures are prepared by thermal evaporation with $Fe_{0.5}Si_{0.5}$ boundary layers grown by coevaporation at 200 °C. Magnetic properties are examined with Brillouin light scattering and longitudinal magneto-optic Kerr effect hysteresis. The interlayer coupling is found to increase in excess of 8 mJ/m^2 by introducing a boundary layer at the bottom interface. The coupling maximum shifts from 7 to 3 Å nominal Si thickness. This effect is related to reduced interdiffusion with the formation of an epitaxial, pinhole-free spacer at smaller thickness. Together with the strong increase of the coupling for decreasing spacer thickness, this results in an enhancement of the coupling. © *2002 American Institute of Physics.* [DOI: 10.1063/1.1499229]

Fe/Si/Fe structures are attracting interest due to strong antiferromagnetic (AF) coupling which is of significance in applications using artificial antiferromagnets and ferrimagnets as, for instance, in magnetic sensors[1] or more recently in antiferromagnetically coupled (AFC) storage media for hard disk drives.[2]

Fe/Si/Fe structures are complex objects for the study of magnetic and transport properties because of the interdiffusion at interfaces with the possible formation of iron silicides of different structure and composition.[3–7] As was shown earlier, Si grown on Fe tends to interdiffuse and to crystallize in epitaxially stabilized CsCl-type, metallic $Fe_{0.5}Si_{0.5}$ (Ref. 3) and exhibits an exponential decay of coupling versus spacer thickness (Refs. 5 and 7). This unusual behavior was related to a new type of exchange coupling across metallic-type spacers[5] in contradiction with the standard quantum interference model (QIM) of interlayer coupling.[8] The QIM predicts an exponential decay of AF coupling only for nonconducting spacers but oscillatory coupling for metallic spacers.

In order to distinguish metallic and insulating-type spacers, we have previously prepared epitaxial $Fe/Fe_{1-x}Si_x/Fe$ trilayers by codeposition of Fe and Si instead of relying on interdiffusion. We achieved a spacer composition close to $Fe_{0.5}Si_{0.5}$ (Ref. 9) and spacers with variable Si content x in the range $0.4<x<1$ (Ref. 10). We deposited $Fe_{0.5}Si_{0.5}$ spacer layers at an elevated temperature (200 °C) in order to form metallic, epitaxial iron silicides and obtained weak oscillatory coupling (less than 1 mJ/m^2).[9] In these samples, the coupling strength increased with decreasing temperature in agreement with the QIM for metallic spacers.[8] Second, we showed that the interlayer exchange coupling strongly increases with the nominal Si content x in epitaxial $Fe_{1-x}Si_x$ spacers exceeding 5 mJ/m^2 for nominally pure Si spacers. With the increase of nominal Si content x, the thickness of the strongest AF coupling (t_{max}) shifted to a smaller Si thickness. We concluded that the very strong coupling (more than 5 mJ/m^2) observed for nominally pure Si spacers is not due to metallic iron silicides, but due to highly resistive, Si-rich spacers.[10] In qualitative accordance with the QIM for insulating spacers, the AF coupling appears to be of short range and increases exponentially with decreasing nominal Si spacer thickness t with a decay length of less than 2 Å.[10] The AF coupling region is limited at the thinner side of the wedges by the onset of ferromagnetic (FM) coupling caused by pinholes.[5,10]

Here, we use codeposited $Fe_{0.5}Si_{0.5}$ boundary layers (BLs) to further reduce interdiffusion and the formation of pinholes at interfaces. A good lattice matching of $Fe_{0.5}Si_{0.5}$ with both Fe and Si enables epitaxial growth of the spacer layer, which is necessary to obtain strong AF coupling.

We grow Fe/Si-wedge/Fe(100) sandwiches in a molecular-beam epitaxy system onto a GaAs(100)/Fe(1 nm)/Ag(150 nm) substrate system.[11] The $Fe_{0.5}Si_{0.5}$ BLs are codeposited from two separate electron-beam evaporators at 200 °C and at low deposition rates (0.1 Å/s) for both Fe and Si. We use calibrated quartz-crystal monitors to control thickness, deposition rates, and relative atomic fluxes. The nominally pure Si spacer thickness t varies from 0 to 20 Å. A 50 Å thick top Fe layer and a 500 Å thick ZnS antireflection coating are deposited at room temperature (RT).

The composition and the structure are controlled *in situ* by Auger electron spectroscopy (AES) and low-energy electron diffraction (LEED). Well-defined LEED patterns at an electron-beam energy of 55 eV are observed throughout the whole structure for $t<7$ Å and indicate epitaxial growth (Fig. 1). For a higher electron-beam energy (300 eV), LEED patterns are observable up to $t\approx 15$ Å for nominally pure Si

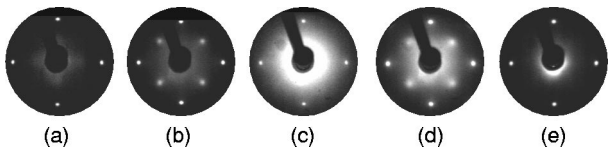

FIG. 1. LEED patterns taken at 55 eV of a structure with two BLs: (a) 50 Å bottom Fe(001) layer, (b) 2.7 Å bottom $Fe_{0.5}Si_{0.5}$BL, (c) 5 Å Si spacer, (d) 2.7 Å top $Fe_{0.5}Si_{0.5}$BL, and (e) 50 Å top Fe(001) layer. Fe and Si layers exhibit the in-plane lattice constant of body-centered-cubic Fe(001) of 2.9 Å. The in-plane lattice constant of the BLs [(b) and (d)] is $\sqrt{2}$ times bigger and therefore allows one to distinguish between $Fe_{0.5}Si_{0.5}$ and nominally pure Si.

[a]Electronic mail: r.gareev@fz-juelich.de

spacers without BLs and up to $t \approx 10$ Å for spacers with BLs. We conclude that the transition to amorphous Si occurs at a smaller thickness in the presence of BLS. The composition of the BLS is calculated from Fe and Si deposition rates as well as from AES spectra. Both methods agree within an error of less than 5% and confirm the composition of the $Fe_{0.5}Si_{0.5}$.[9]

The magnetic properties are examined with longitudinal magneto-optic Kerr effect (MOKE) and Brillouin light scattering (BLS) similar to Refs. 12 and 13, respectively. The external magnetic field of up to $H = 560$ kA/m is applied in the sample plane along an easy axis of Fe. BLS experiments are performed at RT in Voigt geometry using a tandem multipass Fabry–Perot interferometer.

The spin-wave frequencies of optic and acoustic modes are calculated from the spin-wave dispersion relations. The contributions of the bilinear (J_1) and the biquadratic (J_2) terms to the total areal energy density

$$E = -J_1 \cos(\phi) - J_2 \cos^2(\phi),$$

where ϕ is the angle between the film magnetizations, are determined following the formalism described in Ref. 14 by fitting the experimental dependencies of optic and acoustic Stokes and anti-Stokes modes on H for all spacer thicknesses t of interest.

The coupling behavior is examined as a function of t by both MOKE hysteresis and BLS for a set of samples with and without BLS prepared in the same deposition cycle. The frequency of the optic BLS spin-wave mode (F_O) is increasing with the strength of interlayer exchange coupling in contrast to the frequency of the acoustic mode (F_A) which is only sensitive to the alignment of film magnetizations (Voigt geometry for symmetric magnetic layers). Thus, we could determine t_{max} from BLS measurements without switching the two film magnetizations to parallel alignment by an external magnetic field H.

Dependencies of BLS mode frequencies versus H and accordingly calculated values of J_1 and J_2 are presented in Fig. 2 for Fe/Si(t_{max}=7 Å)/Fe and Fe/BL/Si(t_{max}=3 Å)/Fe prepared in the same deposition cycle.

Four regions with different exchange coupling properties can be distinguished from BLS spectra and MOKE hysteresis (Fig. 3). In the first region ($t < t_0$), the coupling is FM and is caused by pinholes ($M_r/M_H = 100\%$ and saturation fields $H_S < 0.1$ kA/m). For spacer thicknesses in the range $t_0 < t < t_{max}$ (region 2), we observe coupling larger than 2 mJ/m^2 with comparable contributions from J_1 and J_2 and a sharp decrease of M_r with t. The strong biquadratic coupling is most likely due to the extrinsic fluctuation mechanism proposed by Slonczewski.[15] In the third region ($t_{max} < t < t_1$), coupling becomes even stronger and preferably AF. This is confirmed by the vanishing remanent magnetization (M_r) in MOKE hysteresis, $H_S \gg 10$ kA/m, and by an abrupt drop of the acoustic mode frequency F_A below F_O. Finally, for $t > t_1$ (region 4), AF coupling becomes negligible and the two film magnetizations align parallel ($F_A > F_O$, $H_S < 0.1$ kA/m, and $M_r/M_H = 100\%$).

Inserting a bottom metallic-type BL leads to a shift of t_{max} from 7 Å down to 3 Å (Fig. 3) and to a significant increase of the interlayer exchange coupling from less than 6 mJ/m^2 to more than 8 mJ/m^2 [Fig. 2 (b)]. In the latter case, the formation of pinholes is strongly suppressed [$t_0 < 1$ Å in Figs. 3(b) and 3(c)]. The smaller width of region 2 of about 2 Å for structures with a bottom BL compared to those without a BL [≈ 4 Å in Fig. 3 (c)] indicates sharper interfaces in the presence of a bottom BL. Magnetic layers with a bottom BL become decoupled for a Si thickness larger than 10 Å (≈ 20 Å without a BL), evidently due to the formation of amorphous Si in the spacer layer[3] which is in good agreement with our conclusion from the structural characterization by LEED. During the deposition of an upper $Fe_{0.5}Si_{0.5}$ BL at 200 °C, the whole structure is annealed. This causes a decrease of the coupling to less than 5 mJ/m^2. Accordingly, the coupling maximum shifts to 5 Å with a wider region 1 of FM coupling ($t_0 \approx 2$ Å). The position of the coupling maximum remains stable upon changing the thickness of the top BL from 1.8 to 3.6 Å with the same extent of region 1 (t_0) of FM coupling.

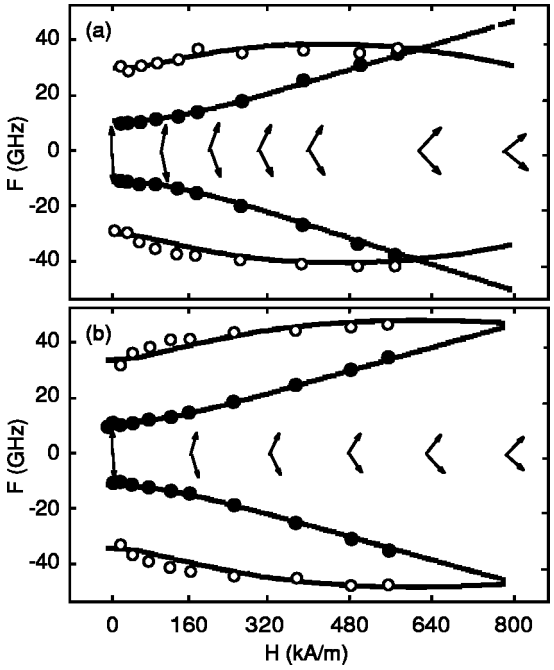

FIG. 2. Spin-wave frequencies of the optic F_O (open circles) and acoustic F_A (filled circles) modes vs magnetic field H for (a) Fe(50 Å)/Si(7 Å)/Fe(50 Å) and (b) Fe (50 Å)/$Fe_{0.5}Si_{0.5}$(2.7 Å)/Si(3 Å)/Fe(50 Å) epitaxial structures prepared in the same deposition cycle. Circles show experimental data and lines fitted curves yielding for (a) $J_1 = -(4.5 \pm 0.5)$ mJ/m^2, $J_2 = -(1.0 \pm 0.1)$ mJ/m^2 and for (b) $J_1 = -(6.6 \pm 0.5)$ mJ/m^2 and $J_2 = -(1.8 \pm 0.2)$ mJ/m^2. Pairs of arrows indicate the directions of the magnetizations of the two films. The Si thicknesses correspond in both cases to $t = t_{max}$. BLS curves are fitted using bulk values for the magnetization (1.7×10^6 A/m) and the magnetocrystalline anisotropy constant (45 kJ/m^3) for both Fe layers.

We qualitatively explained the experimental results as follows: Inserting a bottom BL reduces interdiffusion and thus suppresses the formation of pinholes. As a consequence, AF coupling appears at smaller spacer thicknesses t. Taking into account the established strong increase of AF coupling with decreasing t (Refs. 6 and 10), the strong increase of the coupling in excess of 8 mJ/m^2 (Fig. 2) in the presence of the bottom BL follows in a natural manner. Slightly sharper interfaces, as evidenced by the reduced influence of biquadratic coupling, and a possibly enhanced structural order

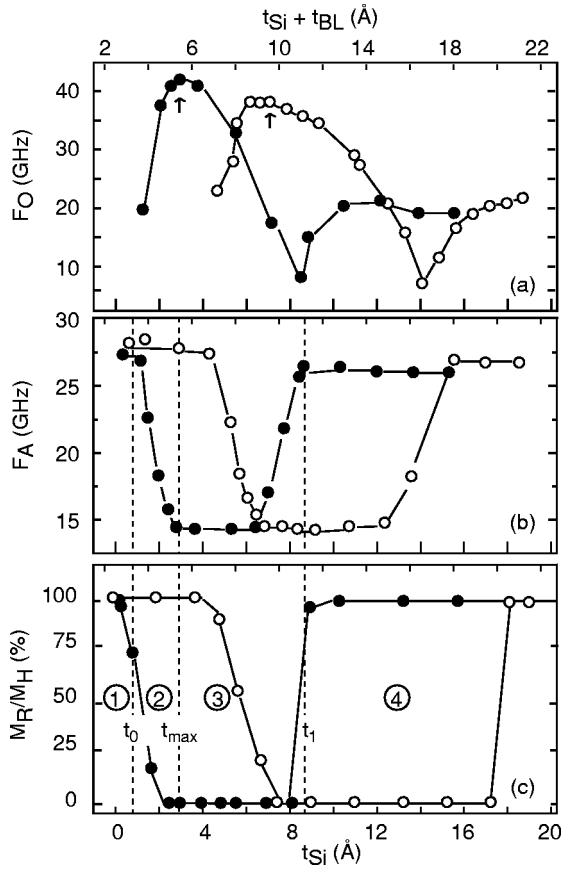

FIG. 3. Frequency shift F_O of the optic (a) and F_A of the acoustic (b) spin-wave modes, and the remanent magnetization M_r/M_H from MOKE (c) vs nominal Si spacer thickness t for Fe(50 Å)/Si(t)/Fe(50 Å) structures with (filled symbols) and without (open symbols) a 2.7 Å $Fe_{0.5}Si_{0.5}$ bottom BL. M_H is measured at $H=560$ kA/m. An external magnetic field $H=160$ kA/m is applied for the BLS measurements. Positions of t_{max} are indicated by arrows in (a). The four coupling regions, t_{max}, t_0, and t_1 are indicated for the structure with BL in (b) and (c). The bottom abscissa corresponds to the nominal Si spacer thickness and the top abscissa to the total thickness of the spacer including the BL. The volume contraction due to the formation of iron silicide (See Ref. 9) in the BL is taken into account.

could also contribute to the stronger coupling. But there is no straightforward explanation as to how they lead to the pronounced shift of the coupling maximum to smaller thicknesses.

In order to understand the microscopic reason of strong AF coupling further work is needed to obtain precise knowledge about the electronic structure, structural order, and the composition of the Si-rich spacer layers.

We conclude that inserting a thin, epitaxial $Fe_{0.5}Si_{0.5}$ BL at the bottom Fe/Si interface in epitaxial Fe/Si/Fe structures results in an enhancement of the interlayer exchange coupling to more than 8 mJ/m^2 despite the increase of the total thickness of the non-magnetic spacer layer. This value of the coupling strength is even larger than for metallic spacer layers. We relate the enhancement of the exchange coupling in the presence of BLs to reduced interdiffusion and slightly sharper interfaces. Therefore, a pinhole-free, Si-rich spacer layer can be grown at an even smaller nominal Si thicknesses compared to Fe/Si/Fe structures without BLs. Together with the established strong increase of the coupling towards smaller thicknesses of nominally pure Si spacers, this results in the observed enhancement of the coupling strength. The concept of using epitaxially stabilized BLs to enhance the AF coupling might also be applicable to other systems that show interdiffusion.

[1] H. A. M. van den Berg, W. Clemens, G. Giers, G. Rupp, W. Schelter, and M. Vieth, IEEE Trans. Magn. **32**, 4624 (1996).
[2] E. E. Fullerton, D. T. Margulies, M. E. Schabes, M. Carey, B. Gurney, A. Moser, M. Best, G. Zeltzer, K. Rubin, and H. Rosen, Appl. Phys. Lett. **77**, 3806 (2000).
[3] A. Chaiken, R. P. Michel, and M. A. Wall, Phys. Rev. B **53**, 5518 (1996).
[4] E. E. Fullerton, J. E. Mattson, S. R. Lee, C. H. Sowers, Y. Y. Huang, G. Felcher, and S. D. Bader, J. Magn. Magn. Mater. **117**, L301 (1992).
[5] J. J. de Vries, J. Kohlhepp, F. J. A. den Broeder, R. Coehoorn, R. Jungblut, A. Reinders, and W. J. M. de Jonge, Phys. Rev. Lett. **78**, 3023 (1997).
[6] Y. Endo, O. Kitakami, and Y. Shimada, Phys. Rev. B **59**, 4279 (1999).
[7] G. J. Strijkers, J. T. Kohlhepp, H. J. M. Swagten, and W. J. M. de Jonge, Phys. Rev. B **60**, 9583 (1999).
[8] P. Bruno, Phys. Rev. B **52**, 411 (1995).
[9] R. R. Gareev, D. E. Bürgler, M. Buchmeier, D. Olligs, R. Schreiber, and P. Grünberg, Phys. Rev. Lett. **87**, 157202 (2001).
[10] R. R. Gareev, D. E. Bürgler, M. Buchmeier, R. Schreiber, and P. Grünberg, J. Magn. Magn. Mater. **240**, 237 (2002).
[11] D. E. Bürgler, C. M. Schmidt, J. A. Wolf, T. M. Schaub, and H.-J. Güntherodt, Surf. Sci. **366**, 295 (1996).
[12] M. Schäfer, S. Demokritov, S. Müller-Pfeiffer, R. Schäfer, M. Schneider, P. Grünberg, and W. Zinn, J. Appl. Phys. **77**, 6432 (1995).
[13] P. Grünberg, in *Topics in Applied Physics*, edited by M. Cardona and G. Güntherodt (Springer, Berlin, 1989), Vol. 66, p. 303.
[14] S. M. Rezende, C. Chesman, M. A. Lucena, A. Azevedo, and F. M. de Aguiar, J. Appl. Phys. **84**, 958 (1998).
[15] J. C. Slonczewski, Phys. Rev. Lett. **67**, 3172 (1991).